Measurement of the Generalized Polarizabilities of the Proton with positron and polarized electron beams

Letter of Intent to Jefferson Lab PAC-51

N. Sparveris (contact: sparveri@temple.edu), H. Atac
Temple University, Philadelphia, PA, USA

M. Jones
Thomas Jefferson National Accelerator Facility, Newport News, VA, USA

M. Paolone
New Mexico State University, NM, USA

and the Jefferson Lab Positron Working Group

(Dated: May 20, 2023)

Abstract

The Generalized Polarizabilities are fundamental properties of the proton, that characterize the system's response to an external quasi-static electromagnetic (EM) field, and have the potential to shed light to key aspects of the structure and dynamics of the proton. They offer a powerful way to study the interplay of the quark and pion-cloud degrees of freedom by revealing how the charge and magnetization distributions inside the system are distorted by the EM field, and they can map out the resulting deformation of the densities in the proton. They provide insight to the underlying dynamical mechanisms e.g. allowing to decode the competing paramagnetic and diamagnetic contributions in the system, and they offer access to important properties such as the proton electric and the magnetic polarizability radius. The GPs have so far been accessed through measurements of the virtual Compton scattering, utilizing an unpolarized electron beam that is scattered from a liquid-hydrogen target. These experiments have accomplished significant advances in recent years, providing high precision benchmark data and valuable guidance to the theoretical calculations, while this activity is expected to continue in the near future. Of special interest are theoretical challenges, in particular with regard to the measurements of the electric polarizability. In this Letter of Intent we propose to follow an alternative experimental path to measure the proton GPs. This will involve measurements with a positron beam, in tandem with measurements with an electron beam, as well as the use of beam polarization. Such an experiment will allow not only to improve upon the precision of the generalized polarizability measurements, but most importantly will provide a much needed critical cross check to the world data, that will be founded on an independent experimental method.

I. INTRODUCTION AND MOTIVATION

The Generalized Polarizabilities are fundamental properties of the proton, that characterize the system's response to an external quasi-static electromagnetic (EM) field. When accessed in real Compton scattering, by measuring the energy and angular distributions of the outgoing photon one can extract the static polarizabilities that quantify the net polarizability effect on the proton [6]. Extending these measurements to the virtual Compton scattering (VCS), the virtuality of the photon allows us to measure the electric and the magnetic generalized polarizabilities, $\alpha_E(Q^2)$ and $\beta_M(Q^2)$ respectively. Their Fourier transform will map out the spatial distribution density of the polarization induced by an EM field and provide a powerful path to study the quark substructure of the nucleon, offering unique insight to the underlying nucleon dynamics. The polarizabilities are sensitive to all the excited spectrum of the nucleon. In describing the GPs through the resulting effect of an electromagnetic perturbation applied to the nucleon components, an electric field moves positive and negative charges inside the proton in opposite directions. The induced electric dipole moment is proportional to the electric field, and the proportionality coefficient is the electric polarizability which measures the rigidity of the proton. The magnetic field acts differently on the quarks and the pion cloud giving rise to two competing contributions, a paramagnetic and a diamagnetic, to the magnetic polarizability. In theoretical calculations, the electric GP α_E is expected to fall-off monotonically with Q^2. The magnetic GP β_M is predicted to have a smaller magnitude relative to α_E, due to the competing paramagnetic and diamagnetic contributions, which largely cancel. Furthermore, it is predicted to go through a maximum before decreasing, as a result of the dominance of diamagnetism due to the pion cloud at small Q^2 and the dominance of paramagnetism due to a quark core at short distances.

In VCS, the measured cross section receives contributions from a number of processes, as shown in Figure 1. Due to electron scattering, one has the Bethe-Heitler process (BH) where the final photon is emitted by the incoming or outgoing electron. The photon electroproduction amplitude is the coherent sum of the Bethe-Heitler, Born and non-Born contributions as shown in Figure 1. The (BH) and (Born) parts, produced due to bremsstrahlung of the electron or proton, respectively, are well known and are entirely calculable with the nucleon EM form factors as inputs, while the non-Born amplitude contains the dynamical internal structure information in terms of GPs. In order to extract the signal of interest from the experimental measurements, one can follow two alternative paths.

The LET (Low energy theorem) [3] provides a path to access these observables analytically. According to the LET, or LEX (Low-energy EXpansion), the amplitude $T^{ep\gamma}$ is expanded in powers of q'_{cm}. As a result, the (unpolarised) $ep \to ep\gamma$ cross section at small q'_{cm} can be written as:

$$d^5\sigma \;=\; d^5\sigma^{BH+Born} \;+\; q'_{cm}\cdot\phi\cdot\Psi_0 \;+\; \mathcal{O}(q'^2_{cm}) \tag{1}$$

where ϕ is a phase-space factor. The notation $d^5\sigma$ stands for $d^5\sigma/dk'_{elab}d\Omega'_{elab}d\Omega_{cm}$ where k'_{elab} is the scattered electron momentum in the lab frame, $d\Omega'_{elab}$ the solid angle of the scattered electron in the lab frame and $d\Omega_{\gamma cm}$ the solid angle of the outgoing photon (or proton) in the p-γ^* CM frame. The Ψ_0 term comes from the interference between the Non-Born and the BH+Born amplitudes at lowest order in q'_{cm}; it gives the leading polarizability effect in the cross section. The LET approach is valid only below the pion production threshold, i.e. as long as the Non-Born amplitude remains real. The Ψ_0 term contains three structure functions P_{LL}, P_{TT} and P_{LT}:

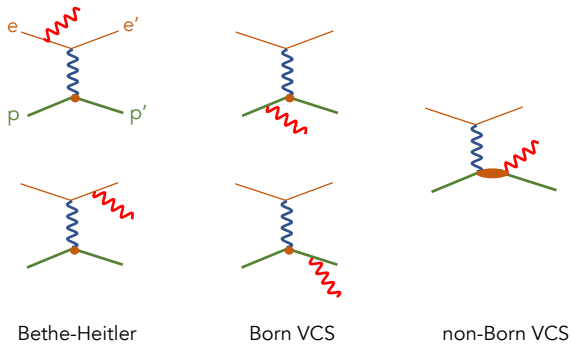

FIG. 1: Diagrams of photon electroproduction, illustrating the mechanisms contributing to ep→epγ. The small circles represent the interaction vertex of a virtual photon with a proton considered as a point-like particle, while the ellipse denotes the non-Born VCS amplitude.

$$\Psi_0 \;=\; v_1 \cdot (P_{LL} - \frac{1}{\epsilon} P_{TT}) \;+\; v_2 \cdot P_{LT} \tag{2}$$

where ϵ is the usual virtual photon polarisation parameter and v_1, v_2 are kinematical coefficients depending on $(q_{cm}, \epsilon, \theta_{cm}, \varphi)$. θ_{cm} and φ are the polar and azimuthal angles of the Compton scattering process in the CM frame of the initial proton and virtual photon. For the structure functions one has:

$$\begin{aligned} P_{LL} &= \tfrac{4M}{\alpha_{em}} \cdot G_E^p(Q^2) \cdot \alpha_E(Q^2) \\ P_{TT} &= [P_{TT\ spin}] \\ P_{LT} &= -\tfrac{2M}{\alpha_{em}} \sqrt{\tfrac{q_{cm}^2}{Q^2}} \cdot G_E^p(Q^2) \cdot \beta_M(Q^2) + [P_{LT\ spin}] \end{aligned} \tag{3}$$

where α_{em} is the fine structure constant and the terms in brackets involves the spin dependent part of the structure functions. The P_{LL} is proportional to the electric GP, and the scalar part of P_{LT} is proportional to the magnetic GP. Using this LET approach one cannot extract all six dipole GPs separately from an unpolarised experiment since only three independent structure functions appear and can be extracted assuming the validity of the truncation to $\mathcal{O}(q_{cm}'^2)$. Furthermore in order to isolate the scalar part in these structure functions a model input is also required.

The sensitivity of the VCS cross sections to the GPs grows with the photon energy and it is thus advantageous to go to higher photon energies. Above the pion threshold the VCS amplitude becomes complex. While T^{BH} and T^{Born} remain real, the amplitude $T^{Non-Born}$ acquires an imaginary part, due to the coupling to the πN channel. The relatively small effect of GPs below the pion threshold, which is contained in $d\sigma_{Non-Born}$, becomes more important in the region above the pion threshold and up to the $\Delta(1232)$ resonance, where the LET does not hold. In this case a Dispersion Relation (DR) formalism is prerequisite to extract the polarizabilities in the energy region above pion threshold where the observables are generally more sensitive to GPs. The DR formalism developed by B.Pasquini et al. [8, 9] for RCS and VCS allows the extraction of structure functions and GPs from photon electroproduction experiments. The calculation provides a rigorous treatment of the higher-order terms in the VCS amplitude, up to the $N\pi\pi$ threshold, by including resonances

in the πN channel. The Compton tensor is parameterised through twelve invariant amplitudes $F_i (i = 1, 12)$. The GPs are expressed in terms of the non-Born part F_i^{NB} of these amplitudes at the point $t = -Q^2, \nu = (s-u)/4M = 0$, where s, t, u are the Mandelstam variables of the Compton scattering. All of the F_i^{NB} amplitudes, with the exception of two, fulfill unsubtracted dispersion relations. These s-channel dispersive integrals are calculated through unitarity. They are limited to the πN intermediate states, which are considered to be the dominant contribution for describing VCS up to the $\Delta(1232)$ resonance region. The calculation uses pion photo- and electroproduction multipoles [10] in which both resonant and non-resonant production mechanisms are included. The amplitudes F_1 and F_5 have an unconstrained part beyond the πN dispersive integral. Such a remainder is also considered for F_2. For F_5 this asymptotic contribution is dominated by the t-channel π^0 exchange, and with this input all four spin GPs are fixed. For F_1 and F_2, an important feature is that in the limit $(t = -Q^2, \nu = 0)$ their non-Born part is proportional to the GPs β_M and $(\alpha_E + \beta_M)$, respectively. The remainder of $F_{1,2}^{NB}$ is estimated by an energy-independent function, noted $\Delta\beta$ and $\Delta(\alpha+\beta)$ respectively. This term parameterises the asymptotic contribution and/or dispersive contributions beyond πN. For the electric and the magnetic GP one gets a similar expression of the following form:

$$\begin{aligned} \alpha_E(Q^2) &= \alpha^{\pi N}(Q^2) + \Delta\alpha \\ \Delta\alpha &= \frac{[\alpha^{exp} - \alpha^{\pi N}]_{Q^2=0}}{(1 + Q^2/\Lambda_\alpha^2)^2} \ . \end{aligned} \tag{4}$$

The two scalar GPs are not fixed by the model, and their unconstrained part is parametrised by a dipole form as shown in eq.(4). This dipole form is arbitrary while the mass parameters Λ_α (and the Λ_β that is equivalently defined for the magnetic polarizability) only play the role of intermediate quantities in order to extract VCS observables. In the DR calculation Λ_α and Λ_β are treated as free parameters, which can vary with Q^2, and their value can be adjusted by a fit to the experimental cross section, separately at each Q^2.

From the theory standpoint, the GPs have been calculated following a variety of approaches, as shown in Fig. 2. In heavy baryon chiral perturbation theory (HBChPT) the polarizabilities are pure one-loop effects to leading order in the chiral expansion [19], emphasizing the role of the pion cloud; the scalar GPs have been calculated to order p^3 [20–22], while the spin GPs have been calculated to order p^4 [23, 24]. The first nucleon resonance $\Delta(1232)$ is taken into account either by local counterterms (ChPT, [19]) or as an explicit degree of freedom (small scale expansion SSE of [22]). In non-relativistic quark constituent models (NRCQM) [3, 25–27] the GPs involve the summed contribution of all nucleon resonances but do not embody a direct pionic effect. The calculation of the linear-σ model (LSM) [28, 29] involves all fundamental symmetries but does not include the Δ resonance, while the effective lagrangian model (ELM) [30] includes resonances and the pion cloud in a more phenomenological way. A calculation of the electric GP was made in the Skyrme model [31]. Recent calculations of the generalized polarizabilities have been performed in baryon chiral perturbation theory [45].

A first group of VCS experiments, at MAMI [11, 12], JLab [13, 14] and Bates [15, 16] that were conducted two decades ago, shaped a first understanding of the proton electric and magnetic GPs. Here, some first experimental evidence that contradict the naive Ansatz of a single-dipole fall-off for $\alpha_E(Q^2)$ were reported, pointing out to an enhancement at low Q^2 evidenced by the MAMI measurements [11, 12]. Two independent experiments [11, 12] were able to confirm this unexpected structure for α_E. The data-analysis of these measurements [11, 12] was later revisited [49, 50], to

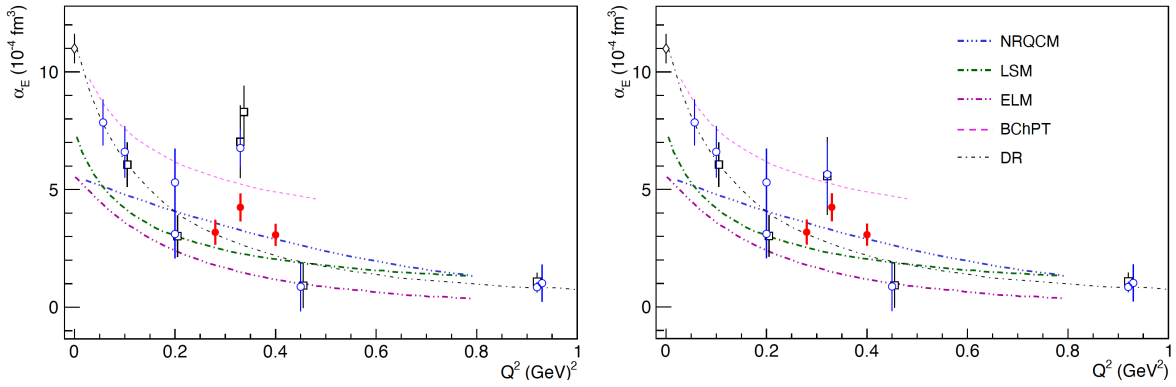

FIG. 2: Left panel: The world data for α_E. The results from the recent JLab VCS-I experiment [2] are shown as filled red circles. Right panel: Same as in the left panel, but with the (un-published) re-analysis of the MAMI data at $Q^2 = 0.33\ GeV^2$ [49, 50]. The theoretical predictions of [25–31, 45] are also shown.

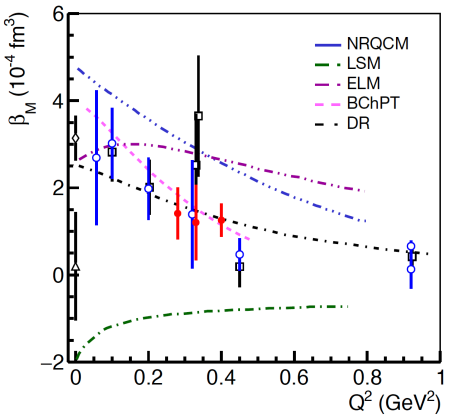

FIG. 3: The magnetic generalized polarizability. The references are the same as in Fig. 2.

account for further refinements in the analysis procedure. The results of this work (as presented in various conferences [49, 50], but currently unpublished) reduces slightly the extracted value for α_E, as shown in Fig. 2 (right panel). A recent generation of experiments (MAMI [42–44] and JLab [2]) improved upon and extended further the measurements of the proton GPs. The world data for the proton GPs are shown in Fig. 2 and in Fig. 3. The experimental data suggest that a non-trivial structure in α_E is likely to exist (currently deviating at the 3σ level from the theoretically predicted monotonic Q^2 dependence). This presents a striking challenge to the current theoretical understanding. The signature of this effect has been explored [2] with phenomenological fits as well as with methods that do not assume any direct underlying functional form [46] (e.g. as shown in Fig. 4(b)). More measurements are needed so as to exclude with higher confidence the possibility that this observation is coincidental. In such a case, the shape and the dynamical signature of this structure needs to be clearly mapped with additional, high precision measurements, so that it can serve as an input for the theory in order to explain the effect. Towards that end, it becomes important to access the proton GPs through an alternative experimental method, so that one can offer an independent confirmation of the observed structure. The scientific merit of conducting measurements of a physics signal by following alternative experimental methods has been illustrated in many occasions in the past. Rather recently, this has been underlined twice in the case of the

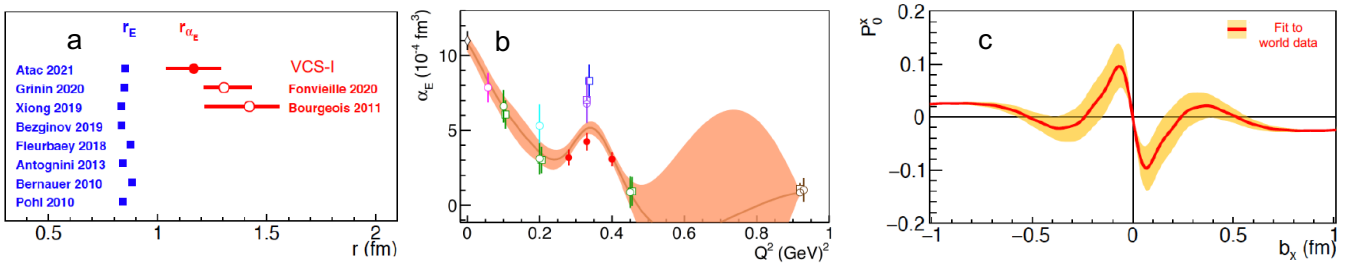

FIG. 4: **a)** The proton electric polarizability radius $r_{\alpha_E} \equiv \sqrt{\langle r^2_{\alpha_E} \rangle}$ is shown in red. The measurements of the proton charge radius are shown for comparison in blue color. **b)** The Q^2-dependence of the electric GP as derived from the experimental measurements using the GPR technique [46], a data-driven method that assumes no direct underlying functional form. **c)** Induced polarization in the proton when submitted to an EM field as a function of the transverse position with photon polarization along the x axis for $b_y = 0$. The x-y defines the transverse plane, with the z axis being the direction of the fast moving protons.

proton, namely in the measurement of the elastic form factors (Rosenbluth vs recoil polarization) as well as in the measurement of the proton charge radius (scattering vs spectroscopy).

Extending the experimental reach of the GP measurements will benefit greatly also on the side of the magnetic polarizability. Here the signal is small, the measurements become more challenging and the relative uncertainties larger, as shown in Fig. 3. Discrepancies between recent experiments [47, 48], highlight further the need to improve our measurements, particularly at low momentum transfers. This is critical towards decoding the processes manifesting in the interplay between diamagnetism and paramagnetism in the proton. A precise mapping of the $\alpha_E(Q^2)$ and $\beta_M(Q^2)$ will further allow to accurately determine the electric and the magnetic polarizability radius of the proton, that is determined from the slope of the electric and the magnetic GPs at $Q^2 = 0$, respectively (e.g. see Fig. 4(a)). The GPs can also be used to describe the spatial deformation of the charge and magnetization densities in the proton [33, 34]. An extraction of the induced polarization in the proton from a fit to the world data [2] is shown in Fig. 4(c). Upcoming experiments can allow to improve this even further, offering a very precise spatial representation of the induced polarization in the proton.

II. PROPOSED VCS ASYMMETRY MEASUREMENTS

The experimental measurements of the proton generalized polarizabilities have so far practically employed unpolarized electron beams. The only exception involves an exploratory measurement of beam spin asymmetries that was conducted in the past [51] at MAMI, but the sensitivity of this experiment to the polarizabilities was extremely limited. Nevertheless, the use of polarized and positron beams provides an alternative and powerful avenue to access the proton GPs. The lepton beam charge (e) and polarization (λ) dependence of the $lp \to lp\gamma$ differential cross section is given by

$$d\sigma^e_\lambda = d\sigma_{\rm BH} + d\sigma_{\rm VCS} + \lambda\, d\tilde{\sigma}_{\rm VCS} + e\,(d\sigma_{\rm INT} + \lambda\, d\tilde{\sigma}_{\rm INT}), \tag{5}$$

where $d\sigma$ ($d\tilde{\sigma}$) are the polarization independent (dependent) contributions which are even (odd) functions of the azimuthal angle ϕ. The $d\sigma_{\rm INT}$ involves the real part of the VCS amplitude that contains the GP effects, while $d\tilde{\sigma}_{\rm INT}$ is proportional to the imaginary part of the VCS amplitude which does not depend on the GPs. Combining lepton beams of opposite charge and different

polarization enables the complete separation of the four unknown INT and VCS contributions. More specifically, using unpolarized electron and positron beams, one can construct the unpolarized beam-charge asymmetry (BCA) A_{UU}^{C} as

$$\begin{aligned} A_{UU}^{C} &= \frac{(d\sigma_{+}^{+} + d\sigma_{-}^{+}) - (d\sigma_{+}^{-} + d\sigma_{-}^{-})}{d\sigma_{+}^{+} + d\sigma_{-}^{+} + d\sigma_{+}^{-} + d\sigma_{-}^{-}} \\ &= \frac{d\sigma_{\rm INT}}{d\sigma_{\rm BH} + d\sigma_{\rm VCS}}. \end{aligned} \tag{6}$$

With polarized lepton beams, on the other hand, one can construct the lepton beam-spin asymmetry (BSA)

$$\begin{aligned} A_{LU}^{e} &= \frac{d\sigma_{+}^{e} - d\sigma_{-}^{e}}{d\sigma_{+}^{e} + d\sigma_{-}^{e}} \\ &= \frac{d\tilde{\sigma}_{\rm VCS} + e d\tilde{\sigma}_{\rm INT}}{d\sigma_{\rm BH} + d\sigma_{\rm VCS} + e\, d\sigma_{\rm INT}}. \end{aligned} \tag{7}$$

The theoretical groundwork and a first theoretical exploration for the potential of this type of measurements has been conducted in [52]. These studies have illustrated that the un-polarized BCA asymmetries and the polarized BSA asymmetries exhibit remarkable sensitivity to both scalar GPs. A combination of both types of assymmetries, such as

$$\begin{aligned} \tilde{A}_{\rm VCS} &\equiv A_{LU}^{+}\left(1 + A_{UU}^{C}\right) + A_{LU}^{-}\left(1 - A_{UU}^{C}\right) \\ &= \frac{2d\tilde{\sigma}_{\rm VCS}}{d\sigma_{\rm BH} + d\sigma_{\rm VCS}}, \end{aligned} \tag{8}$$

and

$$\begin{aligned} \tilde{A}_{\rm INT} &\equiv A_{LU}^{+}\left(1 + A_{UU}^{C}\right) - A_{LU}^{-}\left(1 - A_{UU}^{C}\right) \\ &= \frac{2d\tilde{\sigma}_{\rm INT}}{d\sigma_{\rm BH} + d\sigma_{\rm VCS}} \end{aligned} \tag{9}$$

is powerful towards separating the contribution from the $d\tilde{\sigma}_{\rm VCS}$ and $d\tilde{\sigma}_{\rm INT}$ terms, offering both sensitivity to the GPs as well as a cross-check of the unitarity input in the dispersive formalism, as discussed in [52].

In this Letter of Intent, we capitalize on the work that was performed in [52] and we use it as guidance to conduct a first study on the potential of these measurements using the experimental apparatus that is currently available at Jefferson Lab. Such measurements can be best accommodated in Hall C, using the SHMS and the HMS experimental setup. We first discuss the prospects in conducting measurements of the unpolarized beam-charge asymmetry with electron and positron beams. Our studies have targeted one momentum transfer setting at $Q^2 = 0.35\ GeV^2$ and involve a beam energy of $E_\circ = 2.2\ GeV$. With the SHMS and the HMS measuring $e^{(+,-)}$ and p respectively, we have focused within a range of center of mass energies that exhibits good sensitivity to the polarizabilities, spanning $W = 1150\ MeV$ to $W = 1190\ MeV$. Here, it becomes beneficial to measure out of plane kinematics and the experimental setup offers access at $\phi = 30^o$. We have considered a kinematic range of measurements in $\theta_{\gamma^*\gamma}$ that spans a range as e.g. shown in Fig. 5 for one bin in W. We have considered a scenario of measurements that allows enough statistics so as to bring the statistical uncertainty for each of the (+,-) measurements to the 1%. Here, the uncertainty of the results is already limited by systematic uncertainties. The projected α_E measurement for this set of kinematics is shown at the right panel of Fig. 5. An equally competitive extraction to the

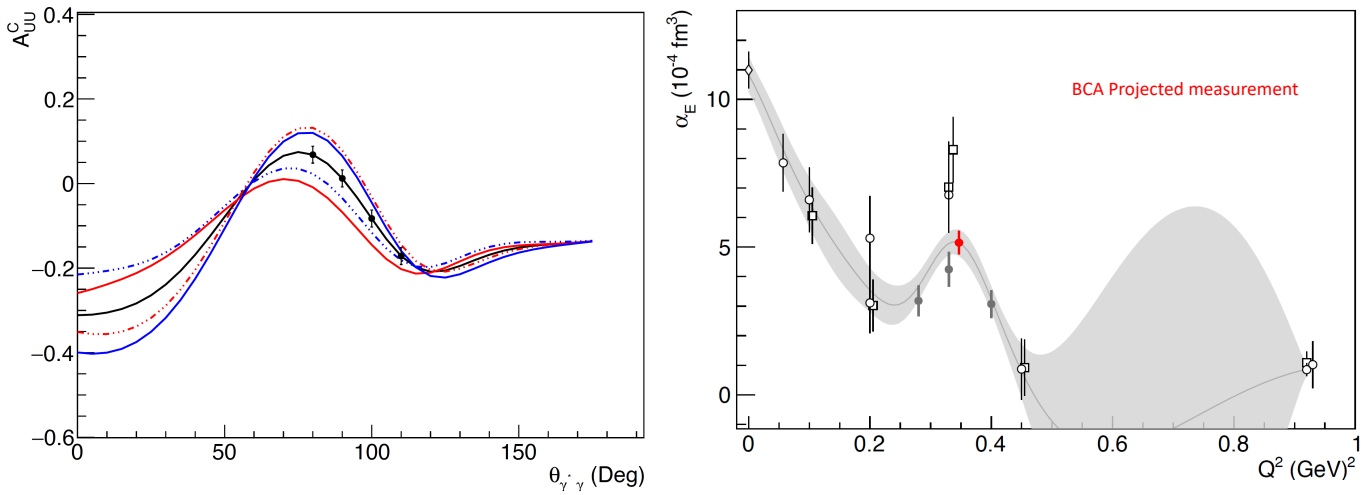

FIG. 5: Beam charge asymmetry measurements with a positron and an electron beam. Left panel: measurements at a fixed bin at $W = 1170\ MeV$ and $\phi = 30^o$. The black curve corresponds to mass scale parameters Λ_α=Λ_β=0.7. The two red (blue) curves explore the sensitivity to the electric (magnetic) GP by varying the Λ_α (Λ_β) from 0.5 to 0.9. Right panel: the projected measurement for the α_E from the BCA measurements is shown in red, along with the world data.

magnetic GP is also projected by these measurements. The group of kinematics with an electron beam requires 1 week of beamtime, with a beam current of $I \sim 50\ \mu A$, depending on the kinematics. The kinematic group counterpart with the positron beam will require more beamtime, since the beam current will be smaller in this case. The exact beamtime will depend on the final performance of the delivered positron beam. The unpolarized positron beam is expected at the level of $\sim \mu A$ level. With an optimistic scenario that one can achieve 5 μA, about 10 weeks of beamtime would be required in such a case for a measurement as shown in Fig. 5. A note can be made here, that since these projections involve measurements that are systematics limited, one could also cut-down the beam-on-target time to some extent, aiming to balance a more economic beamtime request while not inflating significantly the projected uncertainty in the extraction of the polarizability. In this LoI, we have studied and we have presented one potential scenario for such measurements. The studies illustrate the superb potential in accessing the physics of interest through measurements that will employ an unpolarized positron beam. With the endorsement of the PAC, we can plan to extend these studies further towards a complete and comprehensive study of all potential kinematics, that will allow to improve further the precision in the extraction of the polarizability, and will render the beamtime request more efficient.

In the next part, we consider the prospect of using a polarized beam for these measurements. Here, the goal is to measure the beam spin asymmetries (BSA), and these measurements can be conducted independently with either an electron or with a positron beam, without the need to combine the electron and the positron measurements towards the extraction of one measured quantity. Such measurements with a polarized electron beam can become readily available at Jefferson Lab. We present one such scenario of measurements in Fig. 6. We again consider a $Q^2 = 0.35\ GeV^2$ and a beam energy of $E_\circ = 2.2\ GeV$. Here, the sensitivity to the polarizabilities is enhanced at higher center of mass energy, and we consider the range of $W = 1210\ MeV$ to $W = 1250\ MeV$, while the access to out of plane kinematics proves again beneficial. The projected results from such a group of measurements with a $I = 70\ \mu A$ electron beam at 85% polarization is shown in Fig. 6, that will require $\sim$ 2 weeks of beamtime. Here, the beam-spin-asymmetry allows to suppress most of the systematic uncertainties and the statistics become the limitting factor. One can thus run

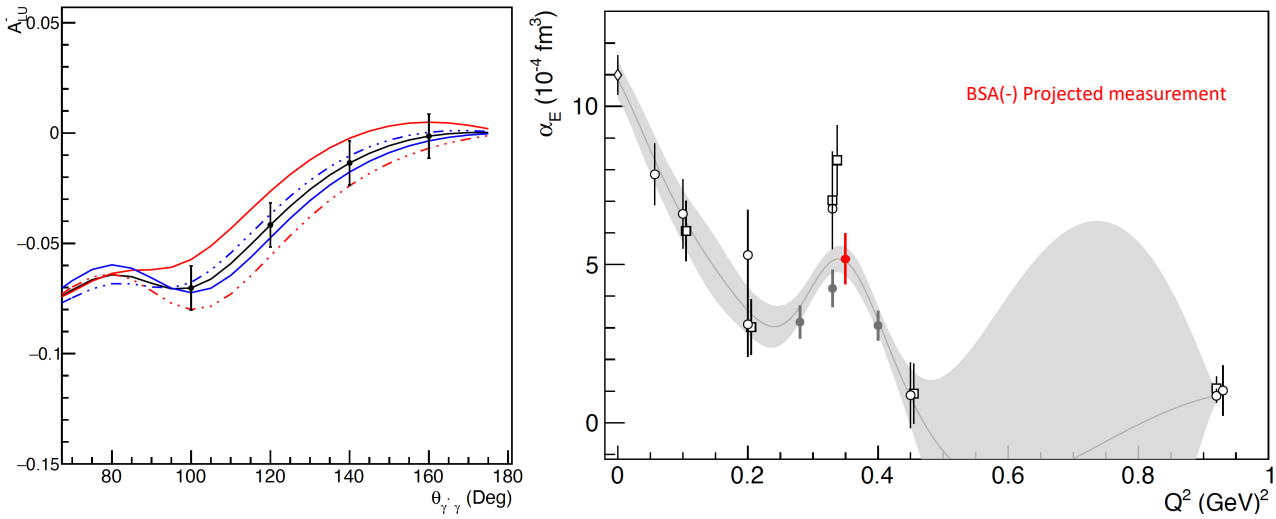

FIG. 6: Beam spin asymmetry measurements with an electron beam. Left panel: measurements at a fixed bin at $W = 1230\ MeV$ and $\phi = 30^o$. The black curve corresponds to mass scale parameters Λ_α=Λ_β=0.7. The two red (blue) curves explore the sensitivity to the electric (magnetic) GP by varying the Λ_α (Λ_β) from 0.5 to 0.9. Right panel: the projected measurement for the α_E from the BSA measurements is shown in red, along with the world data.

additional beamtime so as to further reduce the uncertainties shown in Fig. 6. For comparison, we show the measurements from [51] in Fig. 7, where it is evident that the sensitivity to the GPs where is more limited than in the setup of our measurements. We have also considered the measurement of BSA with a positron beam. For a group of similar measurements (namely, at the same kinematics and of the same precision, as in the case of the electron beam measurements) the sensitivity in the extraction of the polarizabilities is equaly competitive (and slightly better) compared to the measurements with an electron beam. Nevertheless, the issue here involves the beamtime that is needed for such measurements, since the beam current for a polarized positron beam will be significantly suppressed. For example, if one considers an average beam current of $I \sim 50\ nA$ and a beam polarization of 60%, one is facing the need of a beamtime that is 3 orders of magnitude higher compared to the measurements with an electron beam. We consider that this path is not viable, based on the expected performance of a future positron beam at JLab.

III. SUMMARY

We have explored the prospect of studying the proton generalized polarizabilities by following an alternative path compared to what has been employed so far. The use of a positron beam, as well as that of a polarized electron beam, presents a powerful avenue in measuring these fundamental properties of the proton. These measurements will allow to improve further on the measurement of the GPs, will offer the complete separation of the real and imaginary part of the VCS amplitude, as well as a cross-check of the unitarity input in the dispersive formalism. Most importantly, an alternative experimental method will provide a unique cross check to the world-data that have so far been exclusively based on measurements with unpolarized electrons. The scientific merit of conducting measurements of a physics signal by applying alternative experimental methods has been underlined in many occasions in the past. It involves a scientific practice of the highest importance, with the ability to shed light to valuable reaction mechanisms and to enable necessary corrections

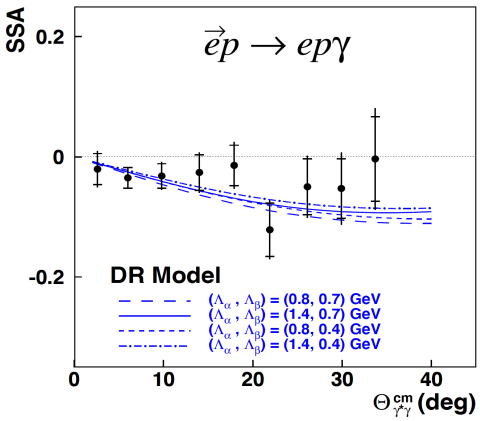

FIG. 7: Figure from reference [51]. The beam SSA in photon electroproduction at $Q^2 = 0.35\ GeV^2$ is compared to the calculation of the DR model for several values of the free parameters Λ_α and Λ_β. The inner error bar is statistical, the outer one is the quadratic sum of statistical and systematic errors.

and improvements to the scientific findings. With this Letter of Intent, we request guidance from the JLab PAC, so that we can pursue this research program with a full proposal. If we receive the endorsement of the PAC, we will be able to proceed with extensive studies in order to identify the kinematics that will offer the optimal balance between the precision in the extraction of the GPs and the requested beamtime, along with comprehensive studies of the background processes and of the systematic uncertainties associated with these measurements. We also note that measurements of the beam spin asymmetries with an electron beam can become readily available at JLab. Such measurments can also be conducted in tandem with future unpolarized VCS experiments (e.g. the proposed VCS-II experiment in Hall C), if the provided beam will be polarized; a fraction of the experimental beamtime can be shared between the two experiments in such a case, thus amplifying the scientific benefit of the awarded beamtime.

[1] H. Fonvieille, B. Pasquini, N. Sparveris, Prog. Part. Nucl. Phys. 113, 103754 (2020)
[2] R. Li, et al., Nature 611, 265 (2022)
[3] P.A.M. Guichon, G.Q. Liu and A.W. Thomas, Nucl. Phys. A 591 (1995) 606.
[4] D. Drechsel, G. Knochlein, A.Y. Korchin, A. Metz, S. Scherer, Phys. Rev. C 57, 941 (1998)
[5] D. Drechsel, G. Knochlein, A.Y. Korchin, A. Metz, S. Scherer, Phys. Rev. C 58, 1751 (1998)
[6] V. Olmos de Leon, et al., Eur. Phys. J. A10 (2001) 207
[7] Pasquini, B. and Vanderhaeghen, M. Dispersion Theory in Electromagnetic Interactions Annu. Rev. Nucl. Part. Sci. 68, 75-103 (2018).
[8] B. Pasquini, M. Gorchtein, D. Drechsel, A. Metz, M. Vanderhaeghen, Eur. Phys. J. A11 (2001) 185-208.
[9] D. Drechsel, B. Pasquini, M. Vanderhaeghen, Phys. Rept. 378 (2003) 99-205.
[10] D. Drechsel, O. Hanstein, S.S. Kamalov, L. Tiator, Nucl. Phys. A 645, 145 (1999)
[11] J. Roche, et al., Phys. Rev. Lett. 85 (2000) 708-711.
[12] P. Janssens, et al., Eur. Phys. J. A37 (2008) 1-8
[13] G. Laveissiere, et al., Phys. Rev. Lett. 93 (2004) 122001
[14] H. Fonvieille, et al., Phys. Rev. C86 (2012) 015210
[15] P. Bourgeois, et al., Phys. Rev. Lett. 97 (2006) 212001
[16] P. Bourgeois, et al., Phys. Rev. C 84 (2011) 035206
[17] MAMI experiment A1/1-09, H. Fonvieille et al, *A study of the Q^2-dependence of the structure functions $P_{LL} - P_{TT}/\epsilon$ and P_{LT} and the generalized polarizabilities α_E and β_M in Virtual Compton Scattering at MAMI.*
[18] MAMI experiment A1/3-12, N. Sparveris et al, *Study of the nucleon structure by Virtual Compton Scattering measurements at the Δ resonance.*

[19] V. Bernard, N. Kaiser, A. Schmidt, U.G. Meissner, Phys. Lett. B 319, 269 (1993) and references therein
[20] T. R. Hemmert, B. R. Holstein, G. Knochlein, S. Scherer, Phys. Rev. D55 (1997) 2630-2643.
[21] T. R. Hemmert, B. R. Holstein, G. Knochlein, S. Scherer, Phys. Rev. Lett. 79 (1997) 22-25.
[22] T. R. Hemmert, B. R. Holstein, G. Knochlein, D. Drechsel, Phys. Rev. D62 (2000) 014013.
[23] C. W. Kao, M. Vanderhaeghen, Phys. Rev. Lett. 89 (2002) 272002.
[24] C.-W. Kao, B. Pasquini, M. Vanderhaeghen, Phys. Rev. D70 (2004) 114004.
[25] G. Q. Liu, A. W. Thomas, P. A. M. Guichon, Austral. J. Phys. 49 (1996) 905-918.
[26] B. Pasquini, S. Scherer, D. Drechsel, Phys. Rev. C63 (2001) 025205.
[27] B. Pasquini, G. Salme, Phys. Rev. C57 (1998) 2589.
[28] A. Metz, D. Drechsel, Z. Phys. A356 (1996) 351-357.
[29] A. Metz, D. Drechsel, Z. Phys. A359 (1997) 165-172.
[30] M. Vanderhaeghen, Phys. Lett. B368 (1996) 13-19.
[31] M. Kim, D.-P. Min (1997) [hep-ph/9704381]
[32] W. Detmold, B. Tiburzi, A. Walker-Loud, Phys. Rev. D 81, 054502 (2010)
[33] A.I. Lvov, S. Scherer, B. Pasquini, C. Unkmeir, D. Drechsel, Phys. Rev. C 64, 015203 (2001)
[34] M. Gorchtein, C. Lorc´e, B. Pasquini, M. Vanderhaeghen, Phys. Rev. Lett. 104, 112001 (2010)
[35] B. Pasquini, D. Drechsel, and M. Vanderhaeghen, Eur. Phys. J. Special Topics 198, 269285 (2011)
[36] H. Fonvieille, Talk at "New Vistas in Low-Energy Precision Physics (LEPP)", Mainz, April 2016; `https://indico.mitp.uni-mainz.de/event/66/session/3/contribution/25/material/slides/1.pdf`
[37] N.D.'Hose, Eur. Phys. J. A28, S01 (2006) 117-127
[38] https://www.jlab.org/Hall-C/upgrade/
[39] https://www.jlab.org/Hall-C/equipment/HMS.html
[40] https://hallcweb.jlab.org/wiki/index.php/Monte_Carlo
[41] N. Sparveris et al, Phys. Rev. C 78, 025209 (2008)
[42] J. Bericic, et al., Phys. Rev. Lett. 123 (2019) 192302
[43] H. Fonvieille, et al., Phys. Rev. C 103 (2021) 025205
[44] A. Blomberg, et al., Eur. Phys. J A 55, 182 (2019)
[45] V. Lensky, V. Pascalutsa, and M. Vanderhaeghen, Eur. Phys. J. C77, 119 (2017).
[46] Rasmussen, C. E., and Williams, C. K. I. Gaussian Processes for Machine Learning the MIT Press, Cambridge Massachusetts, 2006, ISBN 026218253X, ©2006 Massachusetts Institute of Technology
[47] X. Li, et al., Phys. Rev. Lett. 128 (2022) 132502
[48] E. Mornacchi e, et al., Phys. Rev. Lett. 128 (2022) 132503
[49] Fonvieille, H., Conference talk, EINN 2017, Cyprus, (http://2017.einnconference.org/wp-content/uploads/2017/11/EINN-2017-Final-Programme.pdf)
[50] H. Fonvieille, Lecture, *Virtual Compton Scattering*, SFB School 2017, Boppard (https://indico.mitp.uni-mainz.de/event/89/)
[51] I.K. Bensafa et al., Eur.Phys.J.A 32 (2007) 69-75
[52] B. Pasquini and M. Vanderhaeghen, Eur. Phys. J. A 57 (2021) 11, 316